

Supporting information for

Unravelling the key role of surface feature behind facet-dependent photocatalysis of anatase TiO₂

Yung-Kang Peng,^{*a,b} Benedict Keeling,^a Yiyang Li,^a Jianwei Zheng,^a Tianyi Chen,^a Hung-Lung Chou,^c Tim J. Puchtler,^d Robert A. Taylor^d and Shik Chi Edman Tsang^{*a}

^aThe Wolfson Catalysis Centre, Department of Chemistry, University of Oxford, Oxford, OX1 3QR, UK

^bDepartment of Chemistry, City University of Hong Kong, Kowloon Tong, Hong Kong SAR, P. R. China

^cGraduate Institute of Applied Science and Technology, National Taiwan University of Science and Technology, Taipei 10617, Taiwan

^dClarendon Laboratory, Department of Physics, University of Oxford, Oxford, OX1 3PU, UK

Corresponding Author

*edman.tsang@chem.ox.ac.uk

*ykpeng@cityu.edu.hk

EXPERIMENTAL SECTION

Synthesis of 6HF, 2HF and 0HF. 5 mL of $\text{Ti}(\text{OC}_4\text{H}_9)_4$ was mixed with certain amounts of hydrofluoric acid (40–48 w.t%) and distilled water. For the 0HF sample, 6 mL of distilled water was added, for 2HF 2 mL of HF and 4 mL of distilled water were used, whilst for 6HF 6 mL of HF was added in a Teflon-lined autoclave with a capacity of 45 mL, which was then heated to 180 °C for 24h. Following the reaction, any excess liquid was disposed of and the white precipitate was then collected by centrifugation and washed with ethanol and distilled water three times respectively before being dried in an oven at 80°C overnight.

Calcination and NaOH wash for surface F removal. For calcination treatment, 250 mg of as-prepared TiO_2 was calcined under air for 90 min at 600°C at a ramping rate of 5°C min⁻¹. The products were then labelled as Cal-0HF, Cal-2HF and Cal-6HF. For NaOH wash, 250 mg of as-prepared TiO_2 was added to 12.5 mL of 0.1 M NaOH under magnetic stirring for 10h. The solid product was then washed with H_2O and centrifuged three times before drying overnight at 80°C. Samples were then labelled Na-0HF, Na-2HF and Na-6HF.

Photocatalytic hydrogen evolution. 5 mg of catalyst was added to the flask containing 60 mL of distilled water and 40 mL of methanol to act as a sacrificial agent. The vessel was then sonicated before testing and while testing was being conducted, the reaction mixture was constantly stirred using a magnetic stirring bar. Testing was conducted in a closed system with the flask kept at a distance of 45 cm from the UV light source. The system was flushed with nitrogen before testing to remove any oxygen from air. The H_2 produced was determined by using a gas chromatograph.

Photoreduction of Pt on TiO_2 . Pt loading was conducted by impregnation of the above prepared TiO_2 (100 mg) in aqueous H_2PtCl_6 solution (1 wt%), which was freshly prepared by dissolving 2.6 mg of $\text{H}_2\text{PtCl}_6 \cdot \text{H}_2\text{O}$ to 100 mL of water. The mixture was then irradiated under UV light ($\lambda = 365 \text{ nm}$) for 2h at room temperature. The solid precipitate was then filtered and washed several times with EtOH and H_2O and allowed to dry overnight in an oven (80°C).

XPS measurement. XPS measurements were recorded on a Thermo Scientific K-Alfa XPS instrument equipped with micro-focused monochromated Al X-ray source. The source was operated at 12 keV and a 400 μm spot size was used. The analyzer operated at the analyzer energy (CAE) of 200 eV for survey scans and 50 eV for detailed scans. Charge neutralization was applied using a combined low energy/ion flood source. The data acquisition and analysis were conducted with CasaXPS (Casa software Ltd). The peak position was referenced to C1s peak at 285.00 eV.

NMR sample preparation and measurement. 200 mg of TiO_2 sample was placed in a glass tube and removed surface adsorbed water at 150 °C for 2 h under vacuum. After cooling down to room temperature, around 300 μmol /catalyst g of TMP was then introduced. It allowed around 10 min to reach the steady state for adsorption between TMP and catalyst surface. The sample tube was then flame sealed for storage and transferred to Bruker 4mm ZrO_2 rotor with a Kel-F endcap in a glove box under nitrogen atmosphere before NMR characterization. The solid-state MAS NMR measurements were carried out using a Bruker Avance III 400WB spectrometer at room temperature. MAS speed of all our samples was 12 kHz. The high-power decoupling was used for the quantitative ³¹P analysis. During ³¹P NMR experiment, 30° pulse with the width of 1.20 μs , 15 s delay time was adopted. The radiofrequency for decoupling was 59 kHz. The number of scanning was 800. The ³¹P chemical shifts were reported relative to 85% aqueous solution of H_3PO_4 and $\text{NH}_4\text{H}_2\text{PO}_4$ as a secondary standard (0.81 ppm).

Density functional theory (DFT) calculations. Projector-augmented waves (PAW) generalized gradient approximation (GGA) was employed in DFT calculations. In the plane wave calculations, cutoff energy of 500 eV was applied and automatically set by the total energy convergence calculation for anatase $\text{TiO}_2(001)$ and $\text{TiO}_2(101)$ slab system. To calculate the effects of surface fluorine and hydroxyl group to surface Ti chemical states among facets, we placed them on $\text{TiO}_2(001)$ and $\text{TiO}_2(101)$ and calculated the corresponding E_{ad} of trimethylphosphine (TMP) on the given facets. For the modeling of $\text{TiO}_2(001)$ surface, we adopted a slab containing twelve layers of Ti-O units. The surface was constructed as a slab within the three dimensional periodic boundary conditions. The bottom three layers were kept fixed to the bulk coordinates; full atomic

relaxations were allowed for the top nine layers. A suitable dimension of supercell ($11.328 \times 11.328 \times 26.255 \text{ \AA}^3$) was found to perform the adsorption of TMP on $\text{TiO}_2(001)$. Supercell with dimension $10.885 \times 11.328 \times 23.353 \text{ \AA}^3$ was used for $\text{TiO}_2(101)$. The atoms in the cell were allowed to relax until the forces on unconstrained atoms were less than 0.01 eV/\AA . The adsorption energy, E_{ad} , is defined as the sum of interactions between the capping molecule and slab system, and it is given as $E_{\text{ad}} = E_{\text{total}} - E_{\text{TiO}_2(001)} - E_{\text{TMP}}$, where E_{total} , $E_{\text{TiO}_2(001)}$ and E_{TMP} are the energy of total system, $\text{TiO}_2(001)$ slab and TMP molecule, respectively. The calculation of TMP- $\text{TiO}_2(101)$ was carried out similarly. All simulation graphics in this work were generated using GaussView version 3.0.

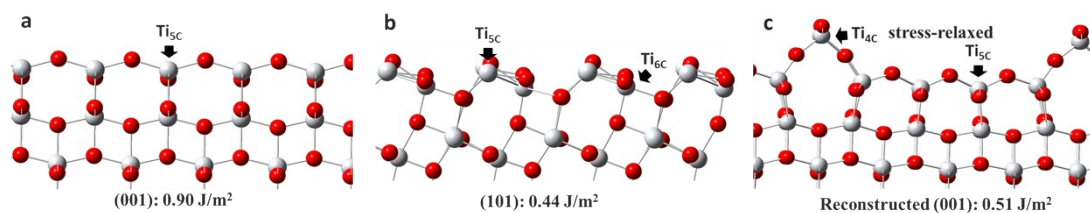
Time-resolved photoluminescence spectroscopy and fitting. Optical characterization was performed using a bespoke micro-photoluminescence setup, in which a frequency-trippled, mode-locked Ti:Sapphire laser ($\lambda = 266 \text{ nm}$, pulse duration = 150 fs , repetition rate = 76 MHz) was directed onto the sample through a $36\times$ reflecting objective (0.5 NA). The excitation spot size was approximately $2\mu\text{m}$. Emission was collected through the same objective before being directed to a 0.3 m spectrometer with a 300 lpmm grating (0.16 nm resolution). Time-resolved measurements were performed using the spectrometer as a monochromator before passing the selected signal to a photomultiplier tube (PMT) detector with an instrument response function width of $\sim 150 \text{ ps}$ connected to a time-correlated single-photon counting module. Parameters describing the photoluminescence were obtained by fitting the background-corrected PL with a biexponential decay function

of the form $y = A_1 e^{-\frac{x}{\tau_1}} + A_2 e^{-\frac{x}{\tau_2}} + y_0$. Errors in the fitting parameters were determined by examining the Adjusted R-squares obtained by independently varying each fitting parameter. For ease of comparison of lifetimes between samples with different quenchers, the intensity average lifetime is defined as

$$\langle \tau \rangle_{\text{int}} = \frac{\sum \alpha_i \tau_i^2}{\sum \alpha_i \tau_i} = \sum_i f_i \tau_i$$

$$f_i = \frac{\alpha_i \tau_i}{\sum \alpha_i \tau_i}$$

where $\frac{\alpha_i \tau_i}{\sum \alpha_i \tau_i}$ is the fractional contribution of each decay component.



Scheme S1. Atomic arrangement of anatase TiO_2 (a) (001) facet, (b) (101) facet and (c) reconstructed (1×4) (001) facet.

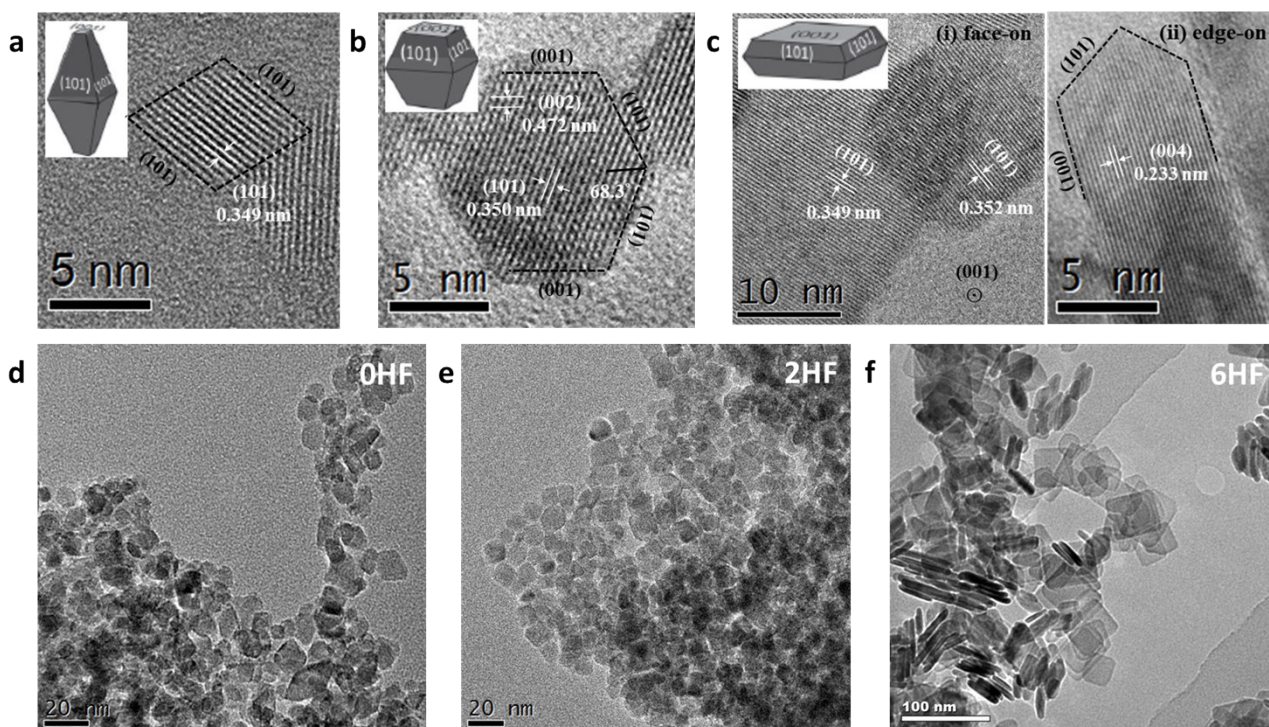


Figure S1. HRTEM images of as-prepared (a) 0HF, (b) 2HF, (c) 6HF. All as-prepared TiO_2 samples exhibited lattice fringes with d-spacings around 0.35, 0.24 and 0.47 nm which correspond to the [101], [004] and [002] crystallographic planar directions of anatase TiO_2 . (d-f) Corresponding TEM images.

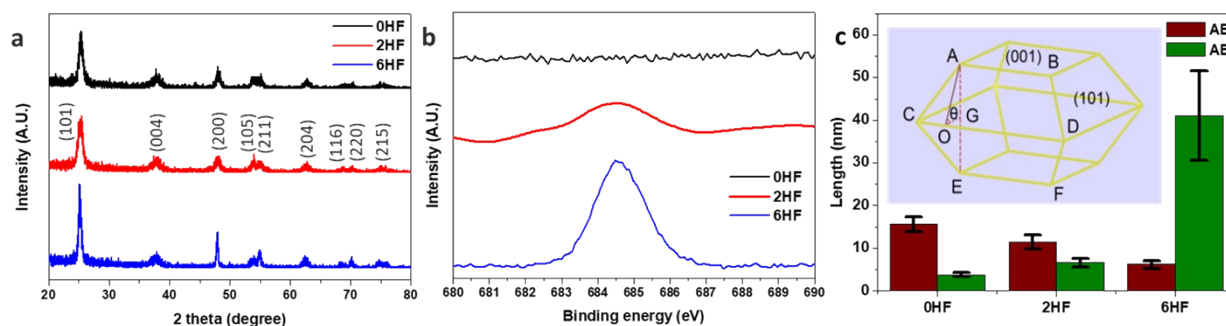


Figure S2. (a) XRD, (b) XPS F_{1s} spectra and (c) statistics on AB (face length) and AE (thickness) values (50 particles are used, see Figure S3 for details) of as-prepared 0HF, 2HF and 6HF samples.

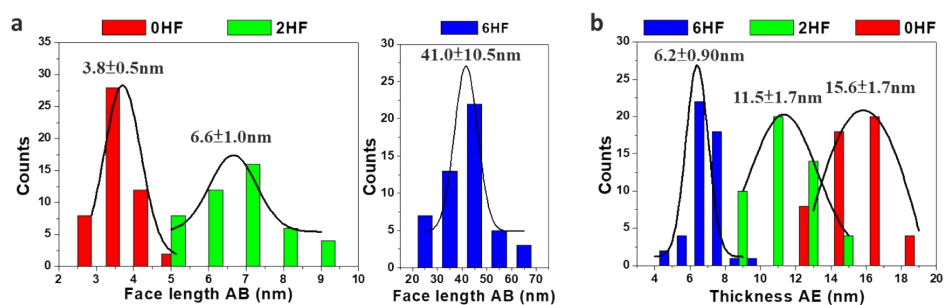


Figure S3. Statistics on (a) side length (AB) and (b) thickness (AE) using simulated shape on 0HF, 2HF and 6HF (50 particles are used for each sample, noted that AB and CD are considered of the same value and θ of 68.3° is the angle between (001) and (101) in the calculation). The 0HF sample gives a shortest face length of 3.8 ± 0.5 nm but widest thickness of 15.6 ± 1.7 nm. For samples prepared with HF, the 2HF sample shows both middle face length (6.6 ± 1.0 nm) and thickness (11.5 ± 1.7 nm), while the 6HF sample displays the longest face length of 41.0 ± 10.5 nm but thinnest thickness of 6.2 ± 0.9 nm.

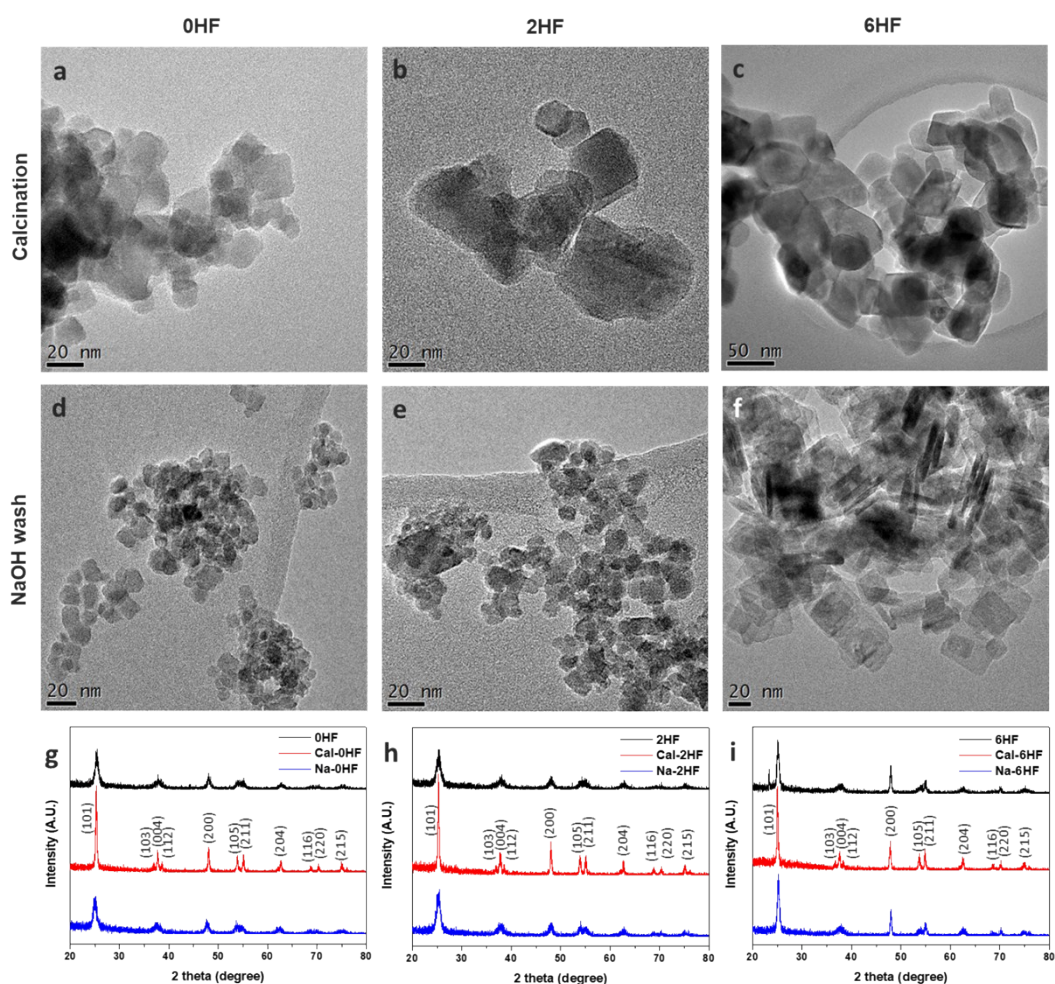


Figure S4. TEM images of TiO_2 samples after calcination treatment (first row): (a) Cal-0HF, (b) Cal-2HF and (c) Cal-6HF and after NaOH wash (second row): (d) Na-0HF, (e) Na-2HF and (f) Na-6HF and (g-i) corresponding XRD spectra.

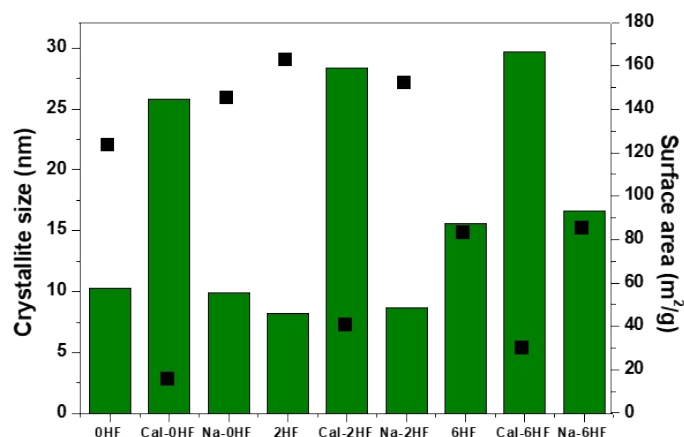


Figure S5. Green bar: crystallite size (nm) calculated from the full width at half-maximum of the (101) peak in Figure S4g-i using Scherrer equation. Black square dot: BET surface area (m²/g) data of 0HF, 2HF, 6HF and their corresponding calcination(Cal-)/NaOH wash(Na-) treatments.

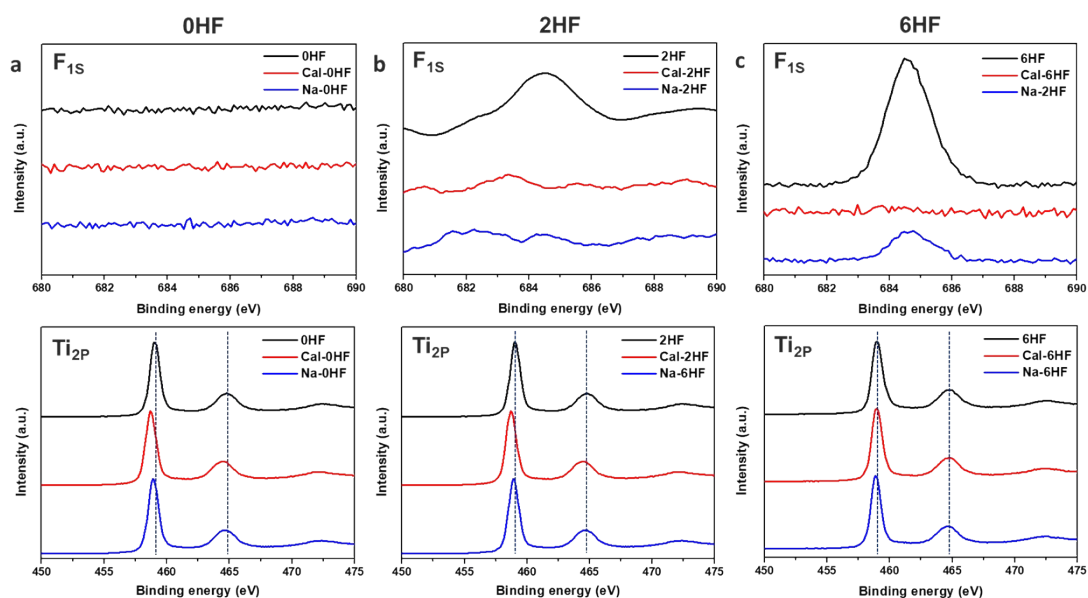


Figure S6. XPS F_{1s} (first row) and Ti_{2p} (second row) spectra of as-prepared (a) 0HF, (b) 2HF and (c) 6HF TiO₂ samples with different treatments (Cal: calcination and Na: NaOH wash). Also see Table S2 for corresponding atomic ratio^[1].

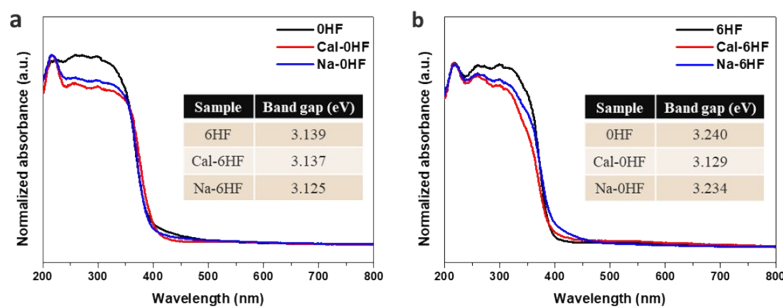


Figure S7. UV-visible measurements of samples with preferential exposed (a) (101) facet (i.e. 0HF) and (b) (001) facet (i.e. 6HF) and their corresponding spectra after calcination(Cal-)/NaOH wash(Na-) treatments. Inset: band gap calculated from Tauc plots.

Discussion on Figure S4-S7

As evidenced by TEM (Figure S4a-c), the calcination treatment causes severe particle aggregation for all calcined samples due to the preferred elimination of high energy (001) facet through the condensation of Ti-OH groups along the [001] crystallographic direction, driven by the minimization of surface energy^[2]. The heat-induced particle aggregation can be further supported by their corresponding XRD and BET measurements. As shown in Figure S4g-i, the sharpening of all XRD peaks (cf. as-prepared faceted TiO₂) with well-resolved (116) & (220) signals and additional (103) & (112) signals clearly indicates that the calcination treatment increases both crystallite size and particle crystallinity. The doubled or even tripled crystallite size calculated from (101) peak for calcined samples also accompanies a large reduction in their corresponding BET surface area (Figure S5). XPS (Figure S6a-c) result suggests the surface F can be completely removed by the calcination treatment, while not for NaOH wash (especially for 6HF sample) presumably due to the reach of equilibrium with NaOH solution. The role of bandgap can also be eliminated as the value is nearly independent with the coverage of (001)/(101) facets and particle size before/after post-treatments on 0HF and 6HF samples (Figure S7).

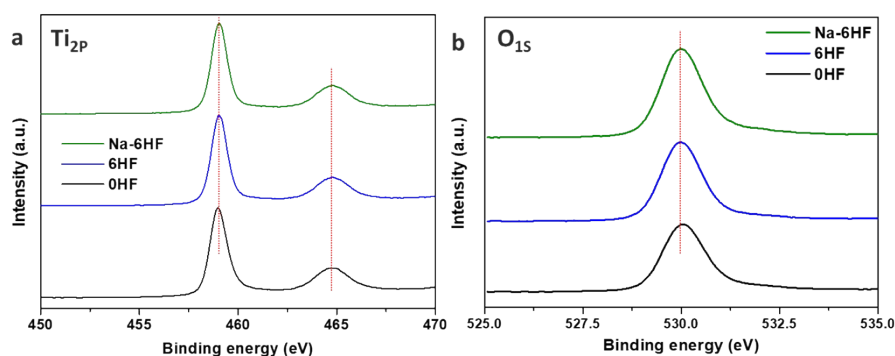


Figure S8. XPS (a) Ti_{2p} and (b) O_{1s} spectra of 0HF, 6HF and Na-6HF samples.

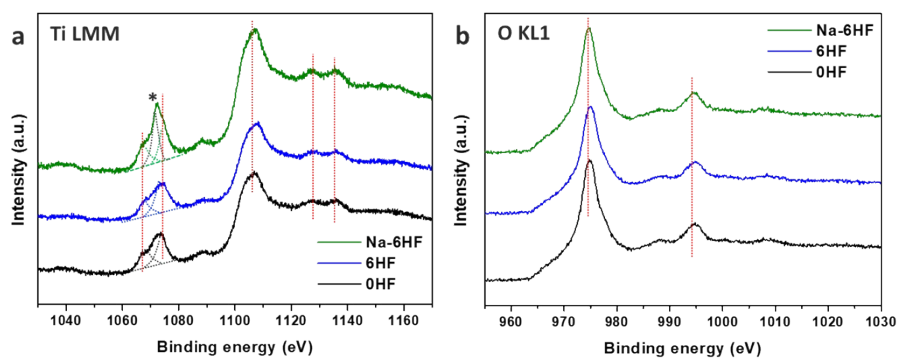


Figure S9. XPS (a) Ti LMM and (b) O KL1 Auger spectra of 0HF, 6HF and Na-6HF samples. The peak marked with asterisk “*” is Na_{1s} signal.

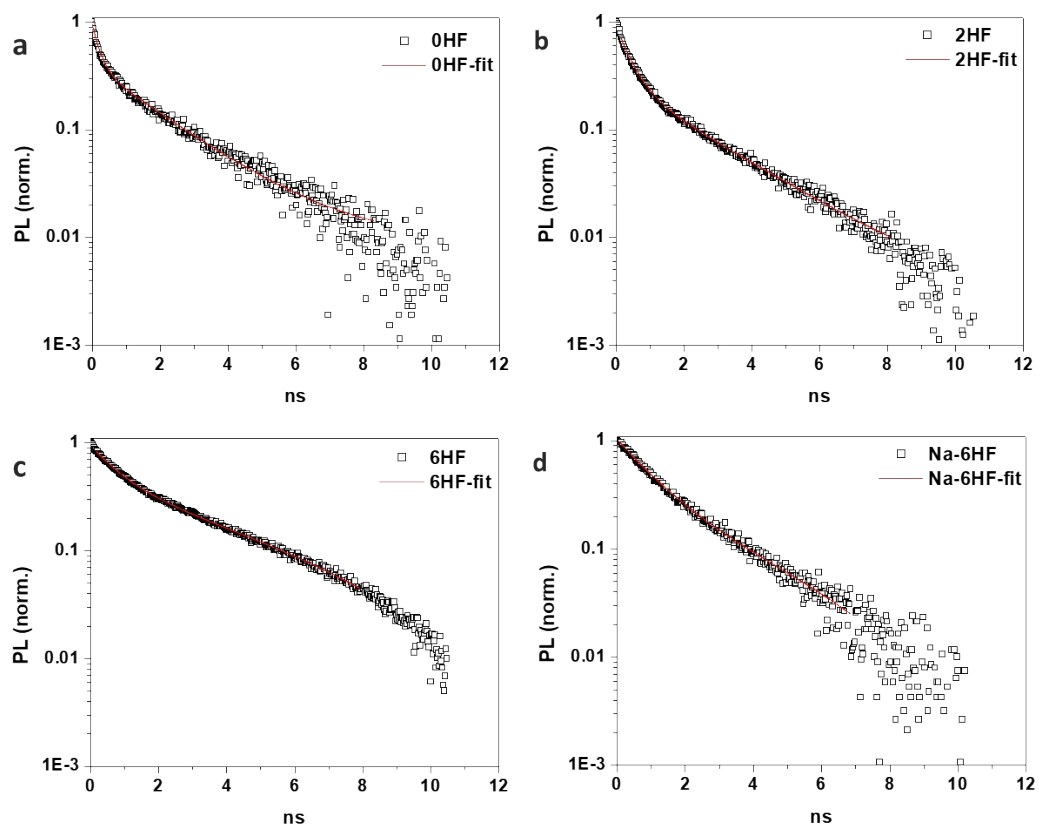


Figure S10. Fitting result of time-resolved photoluminescence of 0HF, 2HF, 6HF and Na-6HF (ns: nanosecond).

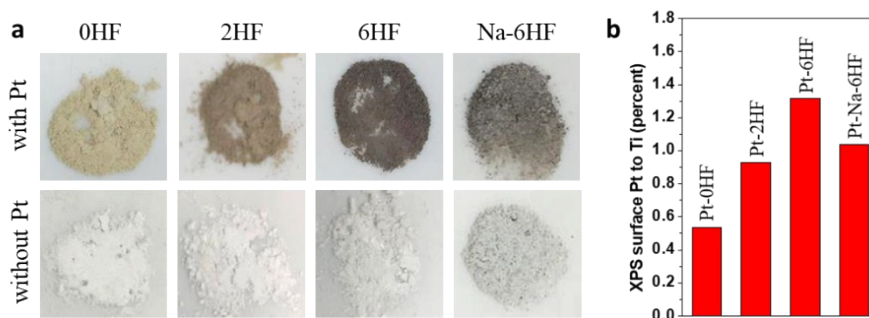


Figure S11. (a) Sample color of 0HF, 2HF, 6HF and Na-6HF before/after Pt deposition and corresponding (b) XPS Pt-to-Ti percentage. The Pt loading was conducted by UV-assisted wet impregnation of TiO₂ sample (100 mg) in aqueous H₂PtCl₆ solution (1 wt%, freshly prepared by dissolving 2.6 mg of H₂PtCl₆•H₂O to 100 mL of water) as widely adopted in literatures.

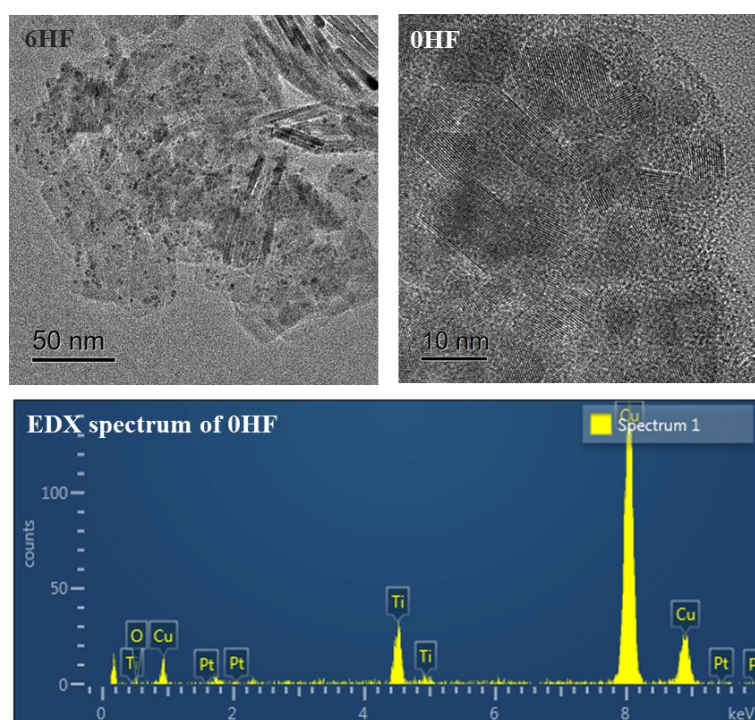


Figure S12. Top: TEM images of Pt loaded 6HF and 0HF. Bottom: energy dispersive X-ray (EDX) analysis of Pt-0HF (Cu signal is the signal from TEM copper grid). Even though no Pt particle for Pt-0HF can be observed by TEM, the existence of Pt element on surface (probably in the form of cluster or atomic dispersion) was confirmed by EDX.

Discussion on Figure S11&S12

As shown in **Figure S11**, the sample color after 1 wt% Pt wet impregnation under UV is clearly different. The darkness of the sample reflects the Pt loading that is believed closely associate with surface fluorine due to the facilitated photo-deposition by the extended exciton lifetime. Indeed, Pt particles size around 2 nm was found on 6HF sample while only small quantity of cluster-size Pt particles (or atomic dispersion) can be found for F-free sample (i.e. 0HF) (**Figure S12**). Despite Na-6HF has similar (001) coverage as 6HF, a lesser degree of darkness of sample color can be clearly observed after NaOH wash. This result strongly suggests the high H₂ activity of (001) facet reported in literatures might due to the difference in Pt particle size and loading rather than its high intrinsic surface energy.

Table S1. Facet-controlled F-capped TiO₂ NPs treated with various post-treatments (Na: NaOH wash; Cal: calcination) and their corresponding activities/mechanisms. F-(001) represents as-prepared F-stabilized TiO₂ NP with preferential exposed (001) facet; Na/Cal-(001) represents F-(001) post-treated with NaOH wash/calcination for the removal of surface fluorine. The key factor proposed by various groups was highlighted and classified into “facet” (yellow) and “surface feature” (green).

Entry	Post-treatment	Reaction	Phase	Activity	Proposed mechanism	Ref. in SI
1	NaOH wash	MO degradation		Na-(001) > F-(001)	Ti _{5C} density on (001) facet	3
2	NaOH wash	MB degradation	molecule in solution	HF-Na-(001) > Na-(001) > F-(001)	surface feature (fluorine)	4
3	Calcination	MB degradation		Increases with (001) coverage (particle with the same size)	Ti _{5C} density on (001) facet	5
4	NaOH wash/ Calcination	MO & MB degradation		MO: F-(001) > Na-(001) ~ Cal-(001) MB: Na-(001) > Cal-(001) > F-(001)	Ti _{5C} density on (001) facet	6
6	-	Acetaldehyde degradation	molecule in air	F-TiO ₂ > TiO ₂	surface feature (fluorine-induced OH)	7
7	NaOH wash	Acetaldehyde degradation		Increases with surface F concentration	surface feature (fluorine)	8
9	NaOH wash	H ₂ evolution	solution is reactant	Na-(101) > F-(101) > F-(001) > Na-(001)	Ti _{5C} density on (001) facet	9
10	NaOH wash	H ₂ evolution	(H ₂ O/CH ₃ OH)	F-(001) > Na-(001) ~ TiO ₂	surface feature (fluorine)	10

Notice that all the cases in **Table S1** are the anatase TiO₂ NPs prepared using fluorine as SDA for the facet control. Accordingly, the NaOH treated (001) facet (i.e. Na-(001)) showed higher activity in the photocatalytic methyl orange (MO) degradation than the as-prepared F-attached (001) facet (i.e. F-(001))^[3], while an opposite result was obtained for the same reaction by the other group^[6] (**Table S1**). Also, the reaction environment seems play a key factor. The post-treated TiO₂ gave higher activity for the degradation of MO^[3] and methylene blue (MB)^[6] than F-attached TiO₂ in aqueous phase, while F-attached TiO₂ showed higher photodecomposition activity than the post-treated TiO₂ toward acetaldehyde^[7,8] in air (**Table S1**). On the other hand, both post treatments (i.e. calcination and NaOH wash) were concluded to increase the facet activity of (101) in photocatalytic hydrogen evolution^[9], while the NaOH wash was reported to lower the activity of (001) in this reaction by others^[9,10] (**Table S1**). In most studies, key factor has been attributed to either “facet” factor (i.e. the higher density of surface Ti_{5C} on (001) than that of (101) from clean model, highlighted in yellow) or “surface feature” factor (i.e. surface fluorine or hydroxyl group, highlighted in green) even adopting the same removal method and catalytic reaction.

Table S2. Comparison of surface information considered in literatures for the correlation of anatase TiO₂ facet activity. *assignment from subsurface TEM lattice spacing. **quantified by using surface area and Wulff construction.

Sample	Dominant Facet*	Surface area (m ² /g)	Quantitative facet distribution**	
			(101) (m ² /g)	(001) (m ² /g)
0HF	(101)	123.3	110.7 (89.8%)	12.6 (10.2%)
2HF	(101)/(001)	163.0	128.6 (78.9%)	34.4 (21.1%)
6HF	(001)	83.0	20.4 (24.6%)	62.6 (75.4%)

Table S3. Atomic ratios of TiO₂ samples evaluated by XPS (Figure S6) with different post-treatments (calcination and NaOH wash)^[1].

0HF	Ti : O : F ratio	2HF	Ti : O : F ratio	6HF	Ti : O : F ratio
0HF	1 : 1.987 : 0.000	2HF	1 : 1.915 : 0.180	6HF	1 : 1.820 : 0.400
Cal-0HF	1 : 1.961 : 0.000	Cal-2HF	1 : 1.980 : 0.000	Cal-6HF	1 : 1.976 : 0.000
Na-0HF	1 : 2.050 : 0.000	Na-2HF	1 : 1.955 : 0.000	Na-6HF	1 : 1.976 : 0.124

Table S4. Time resolved photoluminescence (TRPL) fittings of exciton lifetimes in Figure S10 where f₁ is the fractional component of the first component; f₂ is the fractional component of the second component.

Sample	f ₁	τ ₁ (ns)	f ₂	τ ₂ (ns)	τ _{avg} (ns)
0HF	14.1%	0.21	85.9%	1.92	1.68
2HF	29.4%	0.41	70.6%	2.28	1.73
6HF	15.5%	0.77	84.5%	4.55	3.96
Na-6HF	40.7%	1.01	59.3%	3.60	2.55

Interrelationships between energy facet, surface chemistry and surface impurity and facet-dependent property

It is accepted that the difference in observed facet dependent activity could be rooted from the energy difference in facets. This could give the difference in their surface chemistry such as vacancy formation, electronic structure hence the catalytic properties of the materials. We totally agree with him on this point. Indeed, tailoring the characteristic surface chemistry of nanocrystallite by facet control and hence tuning catalytic activity is a currently key direction.

As mentioned in the introduction section, great effort has been made by researchers looking for suitable structure directing agent (SDA) to kinetically prepare particle terminated with higher energy facet (*Nat. Mater.* **2016**, *15*, 141). However, as many current state-of-the art techniques, such as X-ray photoelectron spectroscopy (XPS) cannot be sensitive enough to reveal the actual change of

chemical state of the surface atom w/o SDA, it is unfortunate that the observed facet dependent activity is simply attributed to corresponding clean higher energy surface model based on the energy argument (the higher energy facet has already been relaxed to other form) without assigning to the actual change in surface chemistry. In addition, the surface impurities introduced during a particular facet preparation can also play a major role in governing catalytic properties. Without a proper analytical tool to monitor the change of surface chemistry during post-treatments and reactions, different interpretations even disagreements about facet activity can often be found among researchers in the past decades (*Nano Today* **2018**, *18*, 15).

Thanks to the newly developed trimethylphosphine(TMP)-assisted ^{31}P NMR technique (*J. Am. Chem. Soc.* **2016**, *138*, 2225), we have showed the relaxation of higher energy anatase TiO_2 (001) facet can be accompanied with its surface reconstruction to lower energy facets or/and the generation of surface features such as oxygen vacancy, hydroxyl group and cation/anion with various chemical states, mainly depending on post-treatments adopted for SDA removal (*Nat. Commun.* **2017**, *8*, 675). Recently, the generation of different types of O species in surface and subsurface with various chemical states during the relaxation of anatase TiO_2 (001) and (101) facets has also been demonstrated by H_2^{17}O -assisted ^{17}O NMR (*Nat. Commun.* **2017**, *8*, 581). The adsorption and further substitution of ^{17}O into the lattice of metal oxides can provide information not only from the surface but also ^{17}O micro-environments in subsurface layers. This facet-dependent adsorption/uptake of H_2^{17}O has also recently observed by ^{17}O NMR on other metal oxides such as CeO_2 (*Sci. Adv.* **2015**, *1*, e1400133) and ZnO (*J. Am. Chem. Soc.* **2016**, *138*, 16322). It is clear from the above literature that the higher energetic facet does not necessary resemble to the corresponding clean higher surface energy model. The relaxation of the higher allergically higher energy facet with the SDA treatment into different surface chemical state may be the principal reason of the higher observed activity. Thus, despite the intensive study of facet-dependent activities of metal oxides in the last two decades, the understanding of the true surface chemistry factor affecting facet activity is still at its infant stage. Clearly, the differences in surface features of anatase TiO_2 (001) and (101) facets with difference treatments (*Nat. Commun.* **2017**, *8*, 675; *Chem. Sci.* **2018**, *9*, 2493) have recently been demonstrated to be the true factor dictating their photocatalytic hydrogen activity.

Here in this manuscript, we have used TMP- ^{31}P NMR to demonstrate that the remaining residue F as a surface impurity on the higher energy (001) facet can exert a strong electric field to prolong the lifetime of excitons, which is the main factor for the enhanced rate of photocatalysis rather than the energy of this facet.

Supplementary References:

- [1] Peng, Y.-K.; Hu, Y.; Chou H.-L.; Fu, Y.; Teixeira, I. F.; Zhang, L.; He, H.; Tsang, S. C. E. Mapping Surface-Modified Titania Nanoparticles with Implications for Activity and Facet Control. *Nat. Commun.* **2017**, *8*, 675.
- [2] Lv, K.; Xiang, Q.; Yu, J. Effect of Calcination Temperature on Morphology and Photocatalytic Activity of Anatase TiO₂ Nanosheets with Exposed {0 0 1} Facets. *Appl. Catal. B* **2011**, *104*, 275–281.
- [3] Han, X.; Kuang, Q.; Jin, M.; Xie, Z.; Zheng, L. Synthesis of Titania Nanosheets with a High Percentage of Exposed (001) Facets and Related Photocatalytic Properties. *J. Am. Chem. Soc.* **2009**, *131*, 3152–3153.
- [4] Yu, X.; Jeon, B.; Kim, Y. K. Dominant Influence of the Surface on the Photoactivity of Shape-Controlled Anatase TiO₂ Nanocrystals. *ACS Catal.* **2015**, *5*, 3316–3322.
- [5] Wu, Q.; Liu, M.; Wu, Z.; Li, Y.; Piao, L. Shape-Controlled Anatase Titanium(IV) Oxide Particles Prepared by Hydrothermal Treatment of Peroxo Titanic Acid in the Presence of Polyvinyl Alcohol. *J. Phys. Chem. C* **2012**, *16*, 26800–26804.
- [6] Liu, S.; Yu, J.; Jaroniec, M. Tunable Photocatalytic Selectivity of Hollow TiO₂ Microspheres Composed of Anatase Polyhedra with Exposed {001} Facets. *J. Am. Chem. Soc.* **2010**, *132*, 11914–11916.
- [7] Jiang, Y.; Scott, J.; Amal, R. Exploring the Relationship Between Surface Structure and Photocatalytic Activity of Flame-Made TiO₂-Based Catalysts. *Appl. Catal. B* **2012**, *126*, 290–297.
- [8] Luan, Y.; Jing, L.; Xie, Y.; Sun, X.; Feng, Y.; Fu, H. Exceptional Photocatalytic Activity of 001-Facet-Exposed TiO₂ Mainly Depending on Enhanced Adsorbed Oxygen by Residual Hydrogen Fluoride *ACS Catal.* **2013**, *3*, 1378–1385.
- [9] Gordon, T. R.; Cargnello, M.; Paik, T.; Mangolini, F.; Weber, R. T.; Fornasiero, P.; Murray, C. B. Nonaqueous Synthesis of TiO₂ Nanocrystals Using TiF₄ to Engineer Morphology, Oxygen Vacancy Concentration, and Photocatalytic Activity. *J. Am. Chem. Soc.* **2012**, *134*, 6751–6761.
- [10] Yu, J.; Qi, L.; Jaroniec, M. Hydrogen Production by Photocatalytic Water Splitting over Pt/TiO₂ Nanosheets with Exposed (001) Facets. *J. Phys. Chem. C* **2010**, *114*, 13118–13125.